geosciences

MDPI

Article

First Calibration and Application of Leaf Wax *n*-Alkane Biomarkers in Loess-Paleosol Sequences and Modern Plants and Soils in Armenia

Yesmine Trigui [1,2,*], Daniel Wolf [1], Lilit Sahakyan [3], Hayk Hovakimyan [3], Kristina Sahakyan [3], Roland Zech [4], Markus Fuchs [5], Tilmann Wolpert [5], Michael Zech [2,6] and Dominik Faust [1]

1 Institute of Geography, Chair of Physical Geography, Technical University of Dresden, Helmholtzstrasse 10, D-01062 Dresden, Germany; daniel_wolf@tu-dresden.de (D.W.); Dominik.Faust@tu-dresden.de (D.F.)
2 Institute of Geography, Chair of Landscape- and Geoecology, Technical University of Dresden, Helmholtzstrasse 10, D-01062 Dresden, Germany; Michael.Zech@mailbox.tu-dresden.de
3 Institute of Geological Sciences, National Academy of Sciences of the Republic of Armenia, Baghramyan Ave. 24a, 0019 Yerevan, Armenia; lilitsahakyan@yahoo.com (L.S.); hghovakimyan@gmail.com (H.H.); sahakyankristina@gmail.com (K.S.)
4 Institute of Geography, University of Jena, Löbdergraben 32, D-07743 Jena, Germany; roland.zech@uni-jena.de
5 Department of Geography, Justus Liebig University Giessen, Senckenberstrasse 1, D-35390 Giessen, Germany; markus.fuchs@geogr.uni-giessen.de (M.F.); Wolpert@geogr.uni-giessen.de (T.W.)
6 Institute of Agronomy and Nutritional Sciences, Soil Biogeochemistry, Martin-Luther University Halle-Wittenberg, von-Seckendorff-Platz 3, D-06120 Halle, Germany
* Correspondence: yesmine.trigui@tu-dresden.de

Received: 13 May 2019; Accepted: 10 June 2019; Published: 17 June 2019



Abstract: Interpreting paleoenvironmental conditions by means of *n*-alkane biomarker analyses is challenging because results depend on different influencing factors. Thus, regional calibration of *n*-alkane patterns is needed because of different plant chemo-taxonomic behavior. We investigated for the first-time leaf wax-derived *n*-alkane biomarkers from modern plants, litter, top soils, and two recently discovered loess-paleosol sequences (LPSs) in Armenia (Lesser Caucasus). Our results on modern samples show a promising discrimination power based on *n*-alkane chain length nC_{33} (probably nC_{31})) for grasses and herbs versus nC_{29} for deciduous trees, despite the large interplant variability within vegetation groups. In contrast with other Loess records in Europe, where Late Pleistocene environments are ranging from tundra-like (glacial) to deciduous forest habitats (interglacial), our results from two Armenian LPSs suggest a transition from humid-steppe biome or forest-steppe vegetation dominating during interglacial periods, to semi-desert shrubs species more adapted to the enhanced aridity during glacial periods.

Keywords: Lesser Caucasus; Armenia; leaf wax biomarker; *n*-alkane; loess; paleosol; Paleo-environment

1. Introduction

Armenia has already reported evidence of climate change over the past years. Future climate projections predict that, because of global warming, the average temperature will further rise by 2–3 °C and rainfall will decrease by 10–15% within the next 50–100 years [1]. This continuous climatic aridification is likely to cause shifts in ecosystems affecting particularly species, which are least tolerant to drought [2] and cause significant negative impacts on agriculture and water resources. To improve our understanding of this critical environmental situation, and to predict the consequences of future climate change, it seems important to intensify investigations on paleoclimate changes and

its paleoenvironmental consequences. During the Quaternary, a series of glacial–interglacial cycles occurred in the Lesser Caucasus region and have played an important role in determining ecosystems and biodiversity of Armenia. However, such climate changes and related environmental impacts have been rarely studied in detail so far. Previous studies on continental deposits often refer to long past Quaternary periods, such as the studies conducted on Quaternary paleo-lake sediments situated near the town of Shamb in southern Armenia [3–5], or to very recent periods (e.g., Leroy et al. [6]). Recently, continuous loess-paleosol sequences (LPSs) were discovered in northeastern Armenia, they are assumed to reflect at least the last three glacial–interglacial cycles [7]. This promising terrestrial archive offers an excellent opportunity to study past Quaternary climate fluctuations and its effects on paleoenvironmental conditions. Wolf et al. [7] have published first stratigraphic results on northeastern Armenian loess sections. In a next step, we aim to use suitable proxy information in order to gather a more detailed paleoenvironmental characterization of these LPSs.

Over the last decades, different proxy-data have been used for obtaining paleoclimatic and paleoenvironmental information from LPSs (e.g., high-resolution grain size data, different weathering indices, or results of organic carbon analyses) [8–11]. However, only very few proxy-data are unaffected by dust accumulation rates that can strongly complicate interpretations [12,13]. Information that can be interpreted largely independent from accumulation rates results from the analysis of leaf wax-derived lipid biomarkers [14–17]. Wax lipids are inherent to all leaves of higher land vegetation and serve as the plant's first barrier from atmospheric interaction, inhibiting the loss of water via evapotranspiration [18–20], and providing ultraviolet light protection to leaf tissue [21]. Among wax lipids, *n*-alkanes became very popular leaf-derived biomarkers because of their relatively high persistence against degradation (insolubility in water and chemical inertness) and their potential to serve as molecular proxies for paleovegetation and paleoclimate reconstruction [22,23]. Extensive research has been devoted to identifying, quantifying, and interpreting leaf wax *n*-alkanes in modern plants, often with the goal of using them for chemotaxonomic fingerprinting. It has been suggested that specific vegetation types produce distinct *n*-alkane patterns. Hence, *n*-alkanes have the potential to indicate vegetation changes, predominantly in terms of differentiating between relative proportions of grasses versus trees (e.g., [24–26]). Regarding *n*-alkane patterns, the homologs C_{27} and C_{29} were identified to generally predominate in leaves of tree and shrub vegetation, whereas the homologs C_{31} and C_{33} were identified to generally predominate in grasses and herbs [17,25,27]. However, a recent study by Bush and McInerney [28], that aimed at testing *n*-alkane patterns in modern plants from all over the world, showed no discrimination power for vegetation reconstruction at a global scale. Therefore, for robustly applying *n*-alkane distributions as paleoenvironmental biomarkers, regional calibration studies based on a survey of *n*-alkane patterns in modern plants and top soils are required.

In this study, we focused on the analysis of *n*-alkane patterns of the drought-adapted vegetation of Armenia (Lesser Caucasus), where lipid patterns neither of recent vegetation samples nor of paleo-vegetation have been described so far. We aimed at testing whether *n*-alkane abundances and chain length distributions are suitable to discriminate between different modern vegetation types and if respective *n*-alkane patterns are likewise transferred to the top soils below.

Moreover, we evaluate the potential of *n*-alkane biomarkers to reconstruct paleo-vegetation and paleoenvironmental conditions based on *n*-alkane patterns in LPSs of northeastern Armenia.

2. Materials and Methods

2.1. Geographical Settings and Sampling

Armenia is a landlocked country located in the southern Caucasus region. About 77% of its area is between 1000 and 2500 m above sea level (a.s.l.) with an average altitude of 1830 m [29]. Its climate ranges from dry sub-tropical to cold alpine. The average annual temperature (1960–2015) is 7.6 °C, varying from −8 °C in the high mountains to 14 °C in low valleys. Armenia receives about 524 mm of precipitation per year (1960–2015). More than 40% of rainfall is concentrated in between April and

June, while the second half of the summer is dry. Low-land areas have mean annual precipitation (MPA) of between 200 and 250 mm, and higher altitudes receive precipitation of between 800 and 1000 mm [2]. Mountain steppes represent the dominant ecosystem of Armenia and occur throughout the country at altitudes between 1200 and 2000 m (sometimes as high as 2500 m). In comparison with other countries of the Lesser Caucasus region, Armenia has fewer forests. Less than 10% of its territory is covered by forests, mostly concentrated in the North-East (62%) and in the South [30], while only 2% corresponds to the central area and the Lake Sevan Basin [2]. Armenian forests are predominantly broadleaved (98.6%), dominated by oak, beech, and hornbeam trees. Dry scrub forests are to be found at altitudes of between 900 and 1000 m in northern parts of the country but occur at much higher altitudes in the southern parts (1800–2000 m). These forests harbor around 80 species of xeric trees and shrubs, all of which are drought tolerant and light-loving [31,32].

The studied loess-paleosol sequences (LPSs) are situated in the northeastern part of Armenia, at the northern flanks of the Lesser Caucasus. All sections are located close to the town of Sevkar north of Ijevan the capital of Tavush province (41° N, 45°10′ E; see Figure 1) at an altitude of between 680 and 960 m a. s. l. These loess deposits form elongated ridges up to 14 m thick, 150 m wide, and 1–2 km long [7].

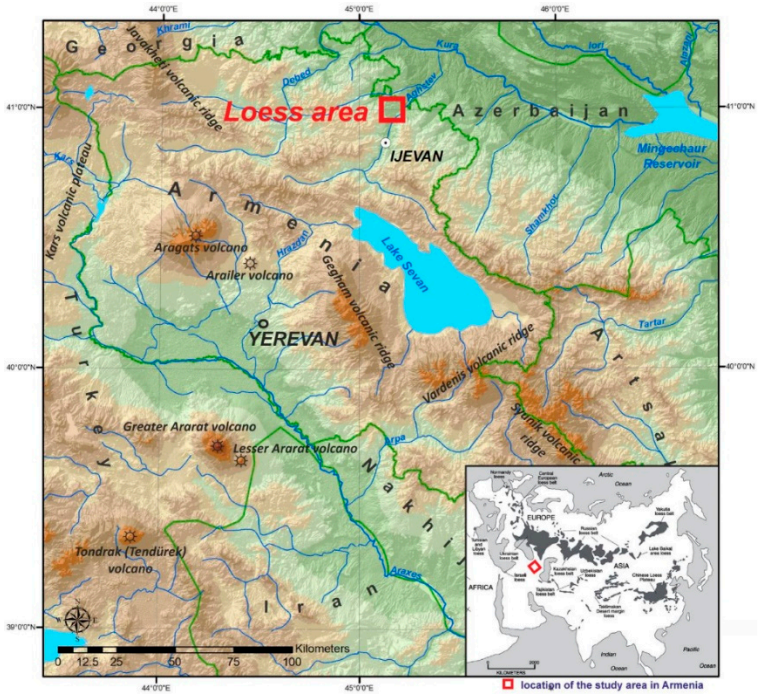


Figure 1. Overview of the study area. The red rectangle marks the loess area near Ijevan, Tavush province NE-Armenia.

The present climate of the loess area is characterized by annual precipitation of between 450 and 550 mm, and a mean annual temperature of about 11 °C. Nowadays, the area is intensively used for agriculture. However, the potential natural vegetation according to recent climate points to forest associations (mesophytic deciduous broad-leaved and mixed coniferous-broadleaved forests) [33]. Accordingly, mesophilic and diversely mixed forests set in as soon as the relief becomes too steep for agricultural activity. A few kilometers to the north, the flanks of the Lesser Caucasus change over into the Transcaucasian depression, a lowland basin that is drained by the Kura River. This transition is related to a natural vegetation change leading over to steppic and dwarf semi-shrub desert plant communities [33]. A spatial shift of this vegetation line, especially during moister or dryer climatic conditions of the late Quaternary period should be considered.

In order to identify late Quaternary vegetation changes in our study area, we investigated two LPSs based on the analysis of leaf-wax derived *n*-alkane patterns. For getting a key to interpret these *n*-alkane patterns, we established a modern reference data set of *n*-alkane patterns. Therefore, we collected 40 samples of fresh plant material as well as six litter samples and six topsoil samples (0–5 cm). Top soils were collected as mixed samples from below the dominant vegetation (2 in grasslands and 4 in sites with deciduous trees/ shrubs). Most sampling sites were situated nearby the studied LPSs in northeastern Armenia, and in the region of Maghavuz in the Republic of Artsakh (Nagorno-Karabakh) where new loess sections were recently discovered. Our approach was to sample plants that are very widespread nowadays, with the assumption that they may have been widespread during similar climate phases in the past as well. As coniferous trees are well known to produce very low *n*-alkane concentrations, which do not contribute significantly to paleo-records [28,34,35], we refrained from sampling and further considering coniferous trees in our approach. For the studies on the LPSs, two loess sections with a thickness of 28 m (Border line (BL) section) and 21 m (Achajur (AJ) section) were selected to carry out *n*-alkane analysis (Figure 2). In total, we took 120 samples from the first section (BL) to include all relevant layers and soil horizons that represent at least three glacial–interglacial cycles [7]. Moreover, we took 40 samples from the well-differentiated upper part of the second profile (AJ) that particularly reflects the last glacial period.

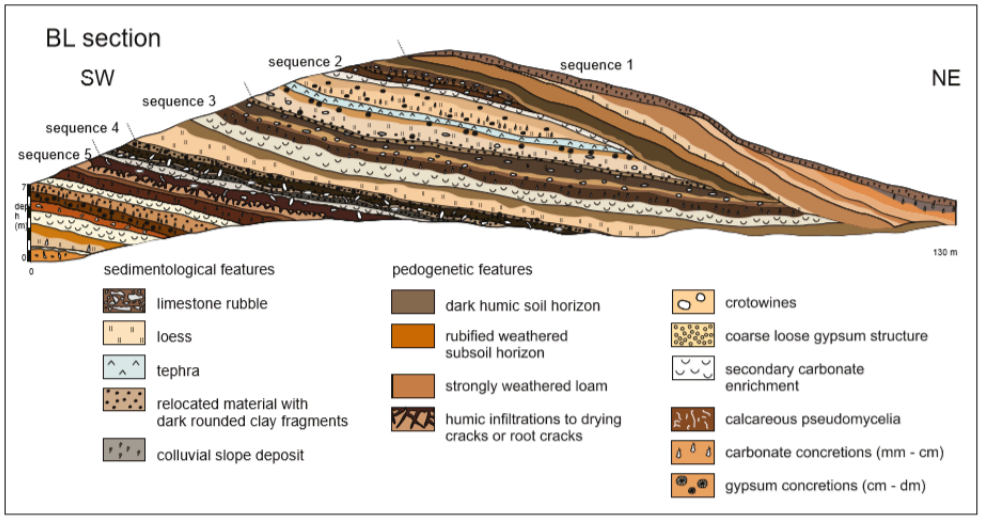


Figure 2. Schematic cross-section of the BL profile. This cross-section relates to a road cut through a loess ridge. The ridge has an elongation of ca. 500 m.

2.2. Stratigraphic Patterns of the Loess-Paleosol Sequences

A detailed description of the BL section is already published in [7]. To introduce the new Achajur (AJ) section, a brief description of the stratigraphic succession is given below. The stratigraphic order of the sedimentation units and the pedo-complexes in the two profile sections were quite similar. They were subdivided into different sequences, which could incorporate loess material, loess-derived soils, soil complexes, colluvial layers, and tephra. From the bottom to the top we differentiated:

- Sequence 5 (17.7–28.5 m in BL profile)

Sequence 5 starts with a thick succession (about 10 m) of strongly weathered dark-brown loams. The occurrence of strong enrichment of secondary carbonate indicates in situ soil formation in the depth of 23.5–26.7 m and 19.8–21.2 m. Each soil is linked to clay contents between 40% and 60% and strong reddish-dark brown to blackish-brown colors. The top of the sequence (until 17.7 m) is characterized by the formation of a blackish soil with high clay contents (>50%), high organic carbon contents (~0.8%), and intense illuviations into drying cracks or root channels.

- Sequence 4 (16–17.7 m in BL profile)

Sequence 4 shows neither strong weathering nor intense loess accumulation. Instead, alternating phases of sediment redistribution and subsequent soil formation occurred, leading to blackish horizons rich in organic carbon (pedocomplex (P-3), after Wolf et al. [7]. In the AJ profile, a definite allocation of Sequence 4 seems too uncertain at the moment.

- Sequence 3 (11.5–16 m in BL profile; 14.7–20 m in AJ profile)

Sequence 3 represents a succession of loess deposits for both profiles, ending up with the formation of another pedocomplex (P-2). Below the P-2 pedocomplex, another weakly developed brownish soil is interposed between the loess layers in both sections. The pedocomplex (P-2) extends from 11.8 to 14.2 m in the BL section and from 15.2 to 18.5 m in the AJ section. The lower part of P-2 starts with a strong blackish-brown soil and pedogenic carbonate enrichment that is more intensely developed in the BL profile. In the upper part of P-2, the BL profile shows a black soil with low clay contents but the highest content of organic carbon in the whole sequence. In contrast, the soil in the upper P-2 in the AJ profile is characterized by strongly weathered reddish-brown material; however, the contribution of slope processes is indicated by numerous clasts and rock fragments. Sequence 3 ends up with a greyish colluvial layer including dark relocated soil material (clay pebbles) that covers the pedocomplex P-2.

- Sequence 2 (5.3–11.5 m in BL profile; 6–14.7 m in AJ profile)

Sequence 2 is characterized by the deposition of thick layers of loess material with low clay contents and bright colors pointing to just limited weathering processes. A pale blueish tephra layer (9.7–10.1 m in BL profile; 12.5–12.9 m in AJ profile) interrupts these loess layers. While in the BL profile the tephra is covered by homogeneous ochre-colored primary loess, the AJ profile clearly points to syn- or post-sedimentary relocation processes that are evidenced by small rock fragments and numerous thin layers of reworked tephra material. In the upper part of sequence 2, a pedocomplex P-1 (Sevkar soil complex) has been formed during marine isotope stage (MIS) 5 as indicated by first OSL-dating [7]. P-1 extends from 5.3 to 7.9 m in BL profile and 6.2 to 9.5 m in AJ profile. It consists of a succession of three palaeosoils and shows a transition from brown clayey soils in the lower part to more blackish and crumby soils in the upper part, which seems quite comparable with the pedocomplex P-2 in the BL profile.

- Sequence 1 (0–5.3 m in BL profile; 0–6m in AJ profile)

Sequence 1 is characterized by a succession of loess deposits with interposed palaeosoils and has been formed during the last glacial (MIS 4 to MIS 2). This sequence shows a very different appearance in both profiles. In general, the loess material seems to be more weathered comparing to the layers below. But in the BL profile, this sequence is divided by two relatively strongly weathered brown soils, while the AJ profile is characterized by up to five weakly-developed and less-intense colored palaeosoils. So far, and without the support by micromorphological analyses, we are not able to identify these soils without a doubt. But it is already evident that, in contrast to the BL profile that experienced most probably two pronounced stability periods during the last glacial, the AJ profile was characterized by stronger sedimentation and relocation dynamics and influenced by less stable conditions. At the top of the sequence, a Holocene soil (P-0) has been developed (0.5–1.5 m in BL profile and 1.3–1.9 m in AJ profile) that is covered by Holocene colluvial deposits in both sections.

2.3. Leaf Wax Analyses and Calculation of n-Alkane Indices

Leaf wax analyses were carried out in the laboratories of the Soil-Biogeochemistry Group of the Martin Luther University in Halle-Wittenberg. Total lipids from modern plants, top soils, and loess sections were extracted with organic solvents DCM:MeOH (9:1), using Soxhlet apparatuses for 24 h. After concentration by rotary evaporation, each total lipid extract was passed over a pipette

column filled with aminopropyl silica gel. The aliphatic fraction, containing the *n*-alkanes, was eluted with 3 mL n-hexane, whereas the polar fraction (e.g., alcohols) and the acid fraction were obtained by DCM:MeOH (1:1) and 5% acid in diethyl ether, respectively. Quantification of the *n*-alkanes was performed on a gas chromatograph coupled to a flame ionization detector (GC-FID). External standards (nC_8–nC_{40}) were run with each sequence for identification and quantification.

Total *n*-alkane concentration (TAC) in plant and soil samples was calculated as the sum of individual *n*-alkane concentrations from nC_{25} to nC_{35} (odd as well as even ones) and was given in µg/g dry weight (dw).

Odd-over-even predominance (OEP) was used as a proxy for degradation and was determined after Hoefs et al. [36]. Low values (<5) indicated an enhanced state of degradation [8,16].

$$\mathrm{OEP} = \frac{\mathrm{nC27} + \mathrm{nC29} + \mathrm{nC31} + \mathrm{nC33}}{\mathrm{nC26} + \mathrm{nC28} + \mathrm{nC30} + \mathrm{nC32}} \quad (1)$$

The average chain length (ACL) of *n*-alkanes, which is the weighted average of the different carbon chain lengths, was calculated by modifying the equation of Poynter et al. [37].

$$\mathrm{ACL} = \frac{27{*}\mathrm{nC27} + 29{*}\mathrm{nC29} + 31{*}\mathrm{nC31} + 33{*}\mathrm{nC33}}{\mathrm{nC27} + \mathrm{nC29} + \mathrm{nC31} + \mathrm{nC33}} \quad (2)$$

The normalized *n*-alkane ratios are:

$$(nC_{31}+nC_{33})/(nC_{27}+nC_{29}+nC_{31}+nC_{33}) \text{ and } nC_{33}/\ (nC_{29}+nC_{33})$$

3. Results and Discussion

3.1. Total n-Alkane Concentrations (TAC), Indices (OEP, ACL), and Patterns of Modern Plants

The investigated samples showed total *n*-alkane concentrations between 29 and 2655 µg/g plant dry weight (dw) (Figure 3a). These values were in the lower to middle range of the interval that has been reported for *n*-alkane concentrations of herbaceous and woody plant species worldwide (0.4–7115 µg/g dw [27,28,34,38–40]). Grasses and herbs produced slightly higher amounts of *n*-alkanes with a mean value of 666 µg/g dw compared to deciduous trees and shrubs, with a mean TAC value of 491 µg/g dw (see Supplementary Materials). For deciduous trees, the highest *n*-alkane concentration was produced by Hawthorn trees (*Crataegus* spp.; 2655 µg/g dw) followed by oak trees (*Quercus* spp.; 1359 µg/g dw) and beech trees (*Fagus* spp.; 651 µg/g dw). The latter two species were the most common ones in Armenian forest communities. The long-chain *n*-alkanes of all investigated modern plant samples revealed a strong odd-over-even predominance (OEP). This is typical for epicuticular leaf waxes of terrestrial higher plants [22]. For deciduous trees and shrubs, about 50% of the samples showed an OEP ranging from 11 to 20, with a minimum value of 8 and a maximum of 30. Grasses and herbs showed quite similar middle values ranging between 9 and 17, with a minimum of 8 and a maximum of 38 (Figure 3b). The OEP is generally considered as a proxy for the preservation status of the leaf-wax derived *n*-alkanes [41–44], with high values being characteristic of not- or just little-degraded *n*-alkanes [34,45]. Thus, OEP values from Armenian plant samples were typical for fresh plant material. The average chain lengths (ACL) of the *n*-alkanes indicated a little difference between the two vegetation groups: Grasses and herbs yielded a slightly higher median value compared to trees and shrubs (Figure 3c). Moreover, nC_{29} and nC_{31} tended to be the most abundant *n*-alkanes in all investigated plant samples (Figure 4a). Our results showed that grasses and herbs generated an equal predominance of both nC_{29} and $nC_{31.}$ However, deciduous trees produced a slightly higher proportion of $nC_{29.}$ In contrast, nC_{33} did not represent a dominant pattern but, overall, was produced in higher amounts by grasses and herbs. In different regions, a predominance of the chained homologs nC_{31} and nC_{33} has been found to be related with herbaceous species [46,47], whereas a higher abundance of the homologs nC_{27} and nC_{29} would be associated with deciduous trees and shrubs [46–48].

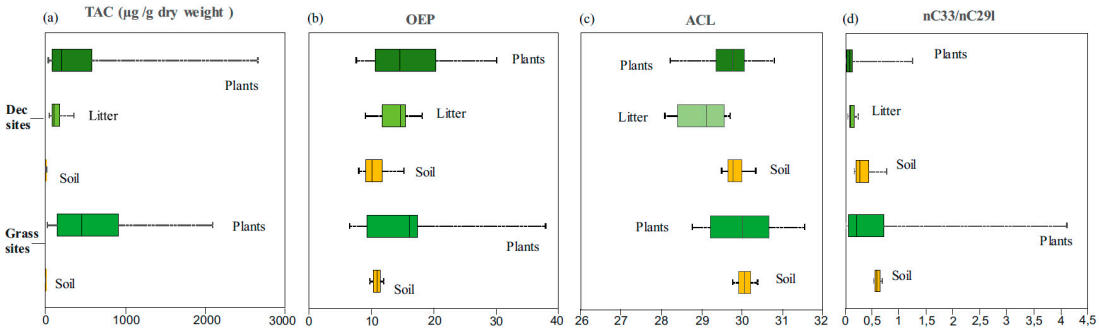


Figure 3. Box plots of *n*-alkane from modern plant and topsoil samples in Sevkar and Maghavuz (Nagorno-Karabakh) regions. (**a**) Total *n*-alkane concertation µg /g (nC_{25}-nC_{35}), (**b**) odd-over-even predominance as degradation proxy (OEP), (**c**) average chain length (ACL), (**d**) *n*-alkane ratio nC_{33}/nC_{29}. Dec sites—sites with deciduous trees and shrubs (n = 22 for plants and n = 4 for top soils). Grass sites—sites with grassland and herbs (n = 18 for plants and n = 2 for top soils). The box plots show median (line inside rectangles), interquartile range (IQR) with upper (75%) and lower (25%) quartiles (full rectangles), and outliers (dashed) lines.

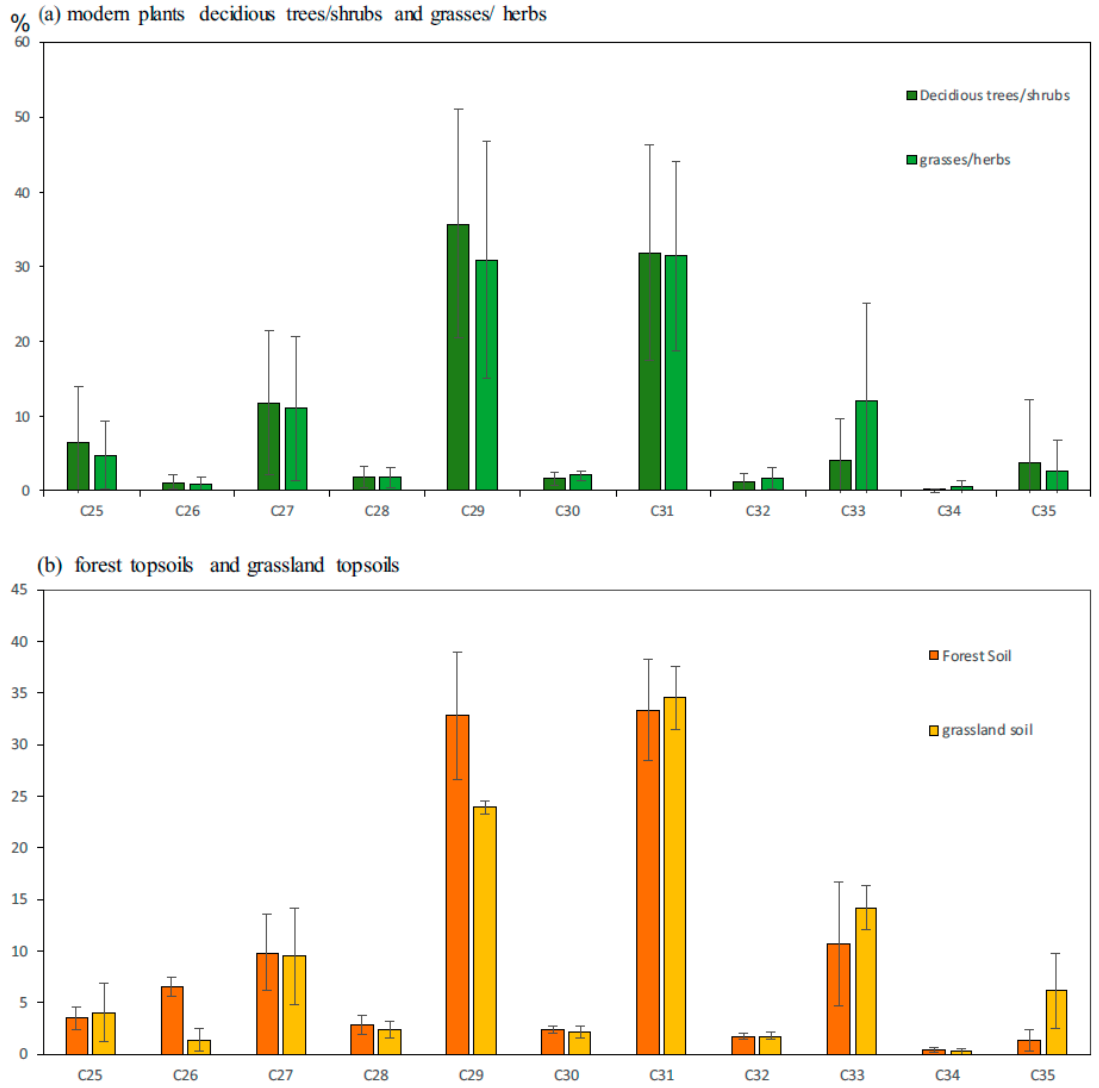


Figure 4. Chain length distribution patterns (%) for long-chain *n*-alkane in (**a**) modern plants (n = 22 for deciduous trees/shrubs, n = 18 for grasses/herbs), and (**b**) top soils (n = 4 for forest, n = 2 for grassland).

Similar patterns are also reported by a recent study conducted in Eastern Georgia [49], a region that is adjacent to our study area. However, such a clear chemotaxonomic character in *n*-alkanes production was not detectable in Armenian modern plant samples. Indeed, likewise in Armenia differences based on C_{33} vs. C_{29} appeared to be a promising tool for differentiating between grasses/ herbs and deciduous trees/shrubs, but this relation is still not confirmed by each sample. This might point to some interplant variability in *n*-alkane production within the same vegetation groups (Figure 3d). Furthermore, we assume that interplant variability and environmental stress may be responsible for the different *n*-alkane patterns between Armenia and Georgia. Nowadays, the climate in NE-Armenia is relatively drier, which represents a stress factor to vegetation and may be expressed in deviating *n*-alkane production. The same observation, albeit with less intensity, has been made in Georgia, where some local hydroclimatic effects and changes in humidity and temperature altered the *n*-alkane patterns of some plants [49]. Indeed, it has been repeatedly discussed in the literature [28,34,50,51] that local environmental conditions and related physiological stress could influence the patterns of *n*-alkane production between members of vegetation groups and within the same species, too. Leaf waxes are the plant's first barrier to the atmosphere. Thus, it is reasonable to hypothesize that their composition, including *n*-alkanes, could be controlled to some degree by environmental adaptation [28,52]. Some species exhibit a high degree of genetic controls over their *n*-alkane patterns, such as the almost exclusive production of nC_{27} by *Fagus sylvatica* leaves [28,53–56], a pattern also confirmed by our analyses to some extent (see Supplementary Materials). In contrast, leaf wax patterns of other plant species may be strongly altered by local environmental parameters, for example temperature and precipitation [37,38,42,56], radiation, nutrient and water availability, salinity, or pollution [52,57].

In a recent study, covering a large set of modern vegetation *n*-alkane data, Bush and McInerney [28] highlighted that the discriminant power based on the chain lengths nC_{27} and nC_{29} vs. nC_{31} and nC_{33} is never better than 75% for any geographical position. For the temperate zone, which also includes Armenia, they even showed that the discriminant power remains only correct for about 49% of the studied woody angiosperm species [28]. Actually, the temperate zone is strongly divided into smaller climate zones, with more variety in temperature and humidity over the year and stronger seasonality changes depending on continentality and highland–lowland effects. In that way, plants may record higher annual and/or monthly variability in produced *n*-alkane patterns, which possibly is demonstrated by the large standard deviations of the *n*-alkanes from modern plant material in Armenia. In view of this high variability within fresh plant material, the analysis of topsoil samples may have the advantage of integrating over the whole ecosystem and implicitly considering such variability [27].

3.2. Total n-Alkane Concentrations (TAC), Indices (OEP, ACL), and Patterns of Litter and Topsoil Samples

The total *n*-alkane concentrations for litter and topsoil samples were 79% and 98% lower, respectively, than those of fresh plant material (Figure 3a). OEP values declined notably from modern vegetation to litter and top soils (Figure 3b), and the ACLs tended to shift towards shorter values (Figure 3c). The considerable decrease in leaf wax *n*-alkane concentrations and OEP values in top soils as compared to fresh plant material were to be expected and indicated effects of degradation and microbial reworking of organic matter (OM) [8,27,58]. The *n*-alkane distribution of forest top soil samples was quite similar compared to leave patterns of deciduous trees and shrubs with both nC_{29} and nC_{31} dominating the sites (Figure 4b). However, in grassland top soils, nC_{31} slightly increased and predominated over the other *n*-alkanes (Figure 4b). In addition, nC_{33}, which is indicative of grasses and herbs as discussed above, tended to be higher in grassland top soils, too (Figure 4b). Thus, there is a tendency to distinguish top soils of grasslands from top soils of deciduous forest sites by a slight predominance of nC_{31} compared to nC_{29}, higher amounts of nC_{33}, and thus slightly higher ACLs values in general (Figure 3c). Such an observation offers a promising base to distinguish between sites that were dominated by grasses and herbs or trees and shrubs (Figure 3d, Figure 4). However, the differences are not high, and this relation should be confirmed by enlarging the data set.

3.3. Total n-Alkane Concentrations (TAC), Indices (OEP, ACL), and Patterns in Armenian Loess-Paleosol Sequences

All samples from the LPSs BL and AJ were characterized by the dominance of long-chain *n*-alkanes with an odd-over-even predominance (OEP), which indicated their leaf wax origin. Total alkane concentrations in both LPSs were relatively low (Figures 5a and 6a) in comparison with other loess areas in Europe, such as the central European loess region [59] and the Carpathian Basin [16,60], where TACs generally exceed 4 µg/g. The reason might be either a lower input (production) or stronger degradation.

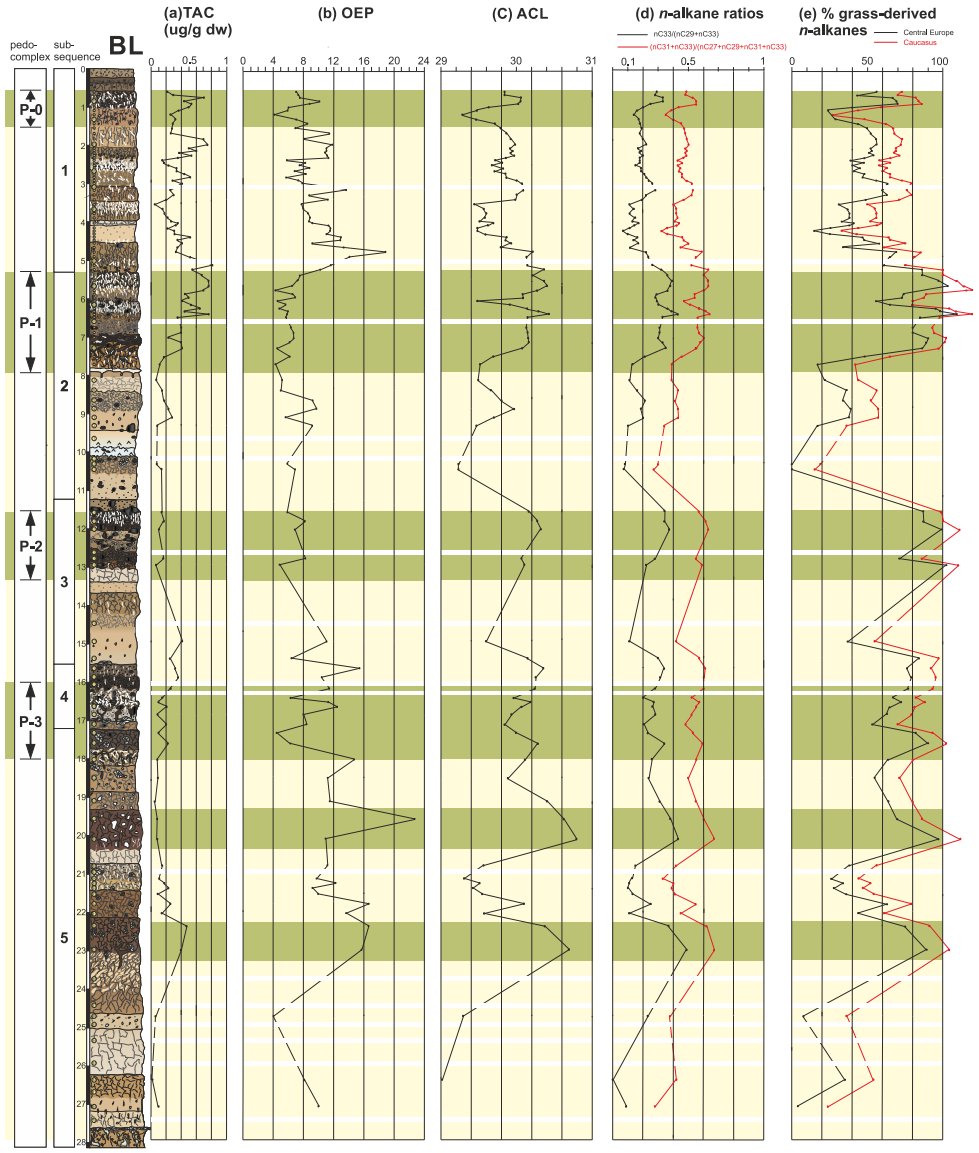


Figure 5. Section of BL profile with differentiation of sub-sequences and pedocomplexes [7]. Depth profiles are sketched for (**a**) total *n*-alkane concentration (TAC µg/g dw), (**b**) odd-over-even predominance (OEP), (**c**) average chain length (ACL), (**d**) *n*-alkane ratios: nC33/(nC29 + nC33) and (nC31 + nC33)/(nC27 + nC29 + nC31 + nC33), (**e**) Percentage of grass-derived *n*-alkane for central Europe and Caucasus models. Sampling points with no available data are indicated with orange bars.

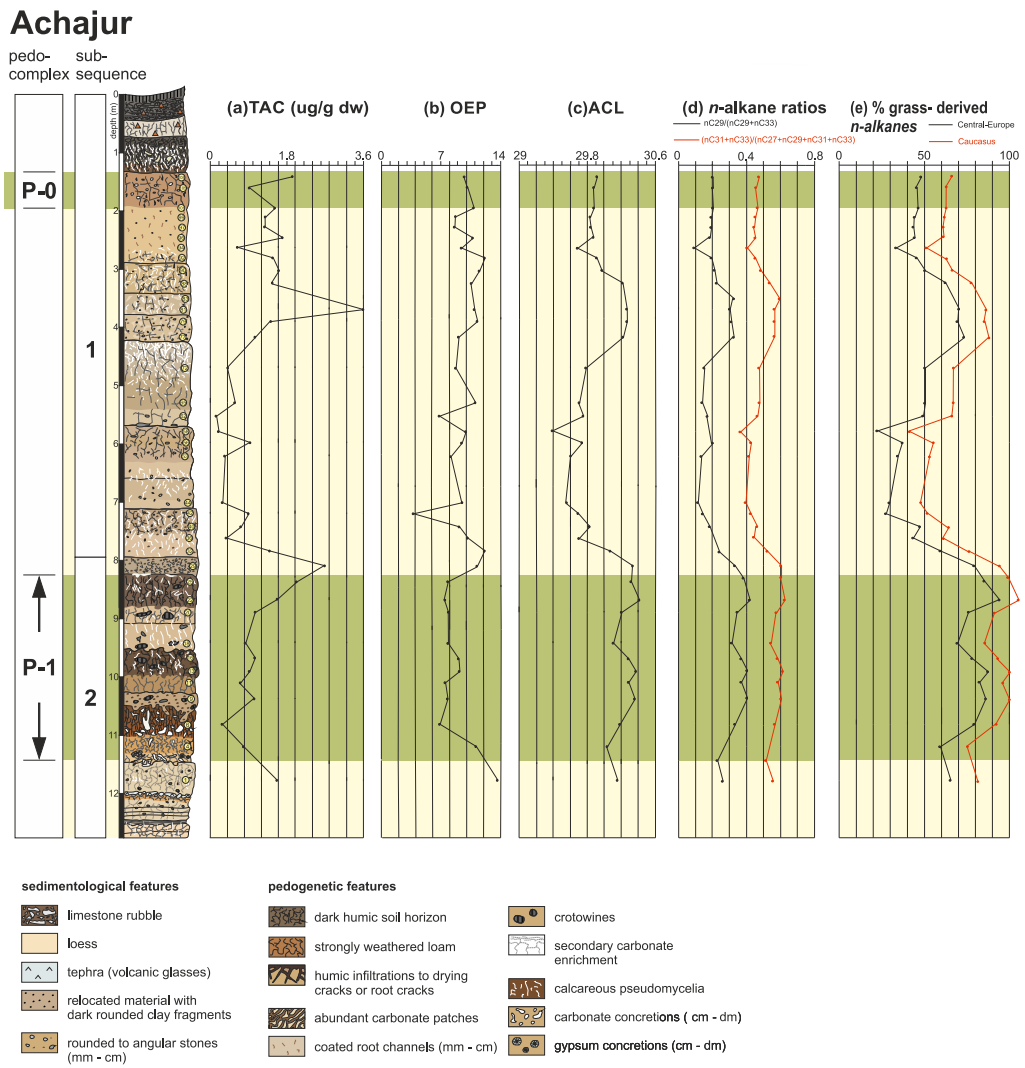


Figure 6. Section of AJ profile with differentiation of sub-sequences and pedocomplexes [7]. Depth profiles are sketched for (**a**) total *n*-alkane concentration (TAC µg/g dw), (**b**) odd-over-even predominance (OEP), (**c**) average chain length (ACL), (**d**) *n*-alkane ratios: nC33/(nC29 + nC33) and (nC31 + nC33)/(nC27 + nC29 + nC31 + nC33), (**e**) percentage of grass-derived *n*-alkane for central Europe and Caucasus models.

The last glacial loess and the soil complex P-1 showed slightly higher *n*-alkane concentrations. An increase in TAC values occurred with the changeover of soil properties within P-1, leading from a brown soil, towards a black-brown soil, and finally to a pure black soil. This might point to a higher bio-productivity or preservation under steppic conditions (Figures 5b and 6b). OEPs along the profiles showed a varying degree of preservation, with lower values pointing to enhanced degradation in some paleo-units. However, there was no general correlation between OEP and TAC. This could be explained by TAC being controlled by both *n*-alkane production and degradation, whereas OEP is primarily controlled by degradation only.

A clear synchronic fluctuation of the average chain length (ACL) and the *n*-alkane ratios $nC_{33}/(nC_{29}+nC_{33})$ and $(nC_{31}+nC_{33})/(nC_{27}+nC_{29}+nC_{31}+nC_{33})$ took place along the studied profiles (Figures 5d and 6d). High values that refer to the predominance of the homologs nC_{31} and nC_{33} were attributable to P-0, P-1, P-2, P-3, a strong blackish soil in the depth of 20 m (BL), and a strongly weathered Kastanozem-like soil at the depth of 23 m (BL). In contrast, a lower ACL and decreased *n*-alkane ratios pointed to the predominance of nC_{29}, which can be mainly associated with glacial periods (e.g., at the depth of 2–5 m, 8–11 m, and ~16 m).

3.4. Paleoenvironmental Reconstruction

As a general tendency in the production of *n*-alkane patterns, the chain lengths nC_{31} and/or nC_{33} are assumed to be predominantly produced by grasses and herbs, while nC_{27} and/or nC_{29} are mainly formed by trees and shrubs. This is suggested by several studies that have been especially undertaken in Central Europe [16,27,59]. Moreover, this discrimination is confirmed by modern *n*-alkane data sets from eastern Georgia as well as promising observations in the study in hand. If we now hypothesize that the pattern in Armenian LPSs follows the same rule, the changes in ACL and the *n*-alkane ratios would suggest that grasses and herbs dominated the ecosystem during the formation of the pedo-complexes (inter-glacial periods), whereas trees and shrubs mainly prevailed during glacial periods (Figures 5 and 6). However, below pedocomplex P-1, concentrations, as well as OEP values, were very low in certain paleo-units. Therefore, it must be considered that just weak changes (e.g., by OM degradation) may result in big changes in the displayed curves.

Although *n*-alkanes are chemically quite inert, various degrading bacteria can utilize them as carbon and energy sources. Thus, the detected signal is probably prone to degradation. Such observations were also discussed by other studies, which highlighted considerable effects of the ongoing degradation of OM in sediments and soils [8,16,17]. In order to prevent misinterpretations and ensure a reliable reconstruction of paleo-vegetation, it seems crucial to minimize possible effects that arise from degradation processes, which could lead to preferential losses of the most dominant alkane homologs. To this objective, Zech et al. [12,16,61] described a correction procedure ("end member model") in more detail. Based on a modern *n*-alkane data set of plant, litter, and topsoil samples from central and southeastern Europe, the model compares the normalized *n*-alkane ratio $(nC_{31}+nC_{33}) / (nC_{27}+nC_{29}+nC_{31}+nC_{33})$ with the OEP to differentiate between vegetation groups and integrate the degradation impact at the same time. In brief, "degradation lines" for *n*-alkanes derived from grasslands and forests are calculated by plotting *n*-alkane ratios against OEP values. Fossil sediments or soil samples formed under grasslands and deciduous forests should plot along the degradation lines of samples from modern data. Furthermore, the contribution of grasses/herbs versus deciduous trees/shrubs to the *n*-alkane signal can be estimated. The percentage of grass vegetation can be calculated by the following formula:

$$\%\ \text{grass} = \frac{\text{n} - \text{alkane ratio (sample)} - \text{equation (degradation line trees)}}{\text{equation (degradation lines grass)} - \text{equation (degradation lines trees)}} * 100 \qquad (3)$$

Grass percentages that exceed 100% illustrate the uncertainties and limitations of the end-member modeling approach because percentages are just semi-quantitative estimations.

Bliedtner et al. [49] integrated *n*-alkane results of modern plant and topsoil samples collected from eastern Georgia into the dataset of Central Europe [59] and recalculated the degradation lines. They further suggest that these adjusted equations could be used to calculate the relative vegetation contributions of grasses vs. deciduous trees in paleo-records from the southern Caucasus and close regions.

After correction, the percentage of grass/herb-derived *n*-alkanes for both the central-European and the adjusted Caucasus models were calculated. (Figures 5e and 6e). Even after correcting the results by taking into consideration OM degradation effects, no major changes were found. Both models showed that it is very likely that herbaceous species were not the predominant source producing *n*-alkanes during the glacial/stadial periods and that deciduous trees and shrubs did not contribute significantly to *n*-alkanes patterns extracted from paleosols. Such findings do not match with the traditional paradigm of the treeless cold steppic environment during glacial conditions and developed deciduous forests in interglacial periods.

3.4.1. "Vegetation Source" versus Environmental Control of Detected n-Alkane Signals

In the same line with recent vegetation patterns, fossil *n*-alkane patterns may also have been controlled by stressful local environmental conditions (e.g., aridity, temperature). Such effects are widely observed in literature and likewise confirmed by the analysis of modern plant material in Armenia. Rinna et al. [61] demonstrated, in a study conducted on marine sediments from the Atlantic and Pacific ocean, that a possible relationship between fossil *n*-alkane chain lengths and latitudinal/altitudinal factors exists. They furthermore suggested that chain lengths of nC_{31}, nC_{33}, and nC_{35} correlate with warmer and drier, or possibly more irradiated environments. In that way, patterns from pedo-complexes in Armenian LPSs pointing to the dominance of nC_{31} and nC_{33} chain lengths might be a response to a stressful environment (e.g., pronounced irradiation or very dry warm summers), boosting the production of the longer *n*-alkane chain lengths nC_{31} and $nC_{33.}$ Likewise, it may be expected that, during glacial conditions, a shortening of the *n*-alkane chain length produced by grasses and herbs may occur due to a decrease in temperature and the enhanced aridity [62]. Thus, the detected fossil *n*-alkane signal could reflect environmental conditions rather than the vegetation source itself.

However, the question remains to which extent stressful environments may globally control the production of *n*-alkane pattern and change plants chemotaxonomic characters based on the predominant formation of nC_{27} and nC_{29} by trees and shrubs and of nC_{31} and nC_{33} by grasses and herbs (see, e.g., [63]).

3.4.2. Deciduous Trees Refugia during Glacial Periods

According to the observed *n*-alkane patterns in the LPSs of NE-Armenia, one could argue that glacial periods in our study area have been linked to tree vegetation, while interglacial periods were characterized by treeless vegetation. Zech et al. [12] experienced similar *n*-alkane patterns in LPSs from the southeastern Carpathian Basin. They attributed such findings to ecologically-effective moisture, suggesting that low soil humidity, as a result of high evapotranspiration during interglacial periods, limited the survival of trees. In contrast, reduced evapotranspiration occurred under cooler climatic conditions favoring tree growth during glacial periods. Thus, it is assumed that parts of southeastern Europe may have served as refugia for deciduous trees during the glacial periods [63,64]. One pivotal question is whether such hydrological relations would be conceivable with respect to our study area in NE-Armenia as well. In general, the interpretation of higher moisture during glacials and drier conditions during interglacials strongly contradicts our interpretation based on stratigraphic and pedogenic results. Based on geomorphological principles, thick unaltered loess layers rather indicate high aridity, while strongly weathered paleosoils that are rich in clay and humic substances evidence more humid conditions.

Further environmental evidence may arise from a comparison with other studies from a regional context. However, such studies are rare in the Caucasus region. Some pollen studies that have been conducted on Early to Middle Quaternary deposits (e.g., Shamb section—paleo-lake sediments in southern Armenia: [3]; North Caucasus and Kazakhstan: [65]) have suggested that the Pleistocene climate was characterized by an alternation of wet conditions during glacial periods and dry conditions during interglacial periods. Other, more modern pollen studies based on precise chronologies (Shamb section in southern Armenia: [5]; Dmanisi (Georgia): [66]; Lake Urmia (NW-Iran): [67]; Lake Van (Eastern Turkey): [68,69]) contradict this interpretation and suggest that glacial periods have been dry and cold and predominantly linked to a vegetation cover composed of grasses and herbs. In view of the high heterogeneity of hydrological conditions during glacial–interglacial cycles that must be expected for the mountainous Caucasus region, a comparison with these faraway paleoenvironmental archives will probably not lead to reliable statements. For this purpose, the analysis of a considerably closer Quaternary archive, such as the Lake Sevan in central-eastern Armenia would be needed. This also means that, for the moment, we have hardly any comparative information and all indications regarding paleoenvironmental conditions originate from the LPSs themselves.

One important hint on vegetation cover appears in the lowermost paleosoil of pedocomplex (P-1) that corresponds to the last interglacial period. Here, up to 5 cm thick root channels have been refilled with clay–humic material indicating the prevalence of tree vegetation. Moreover, the largely unaltered loess units contain no expressions of higher moisture during glacial periods. Low clay contents, low organic contents and bright colors [7] point to mostly absent weathering dynamics that, in turn, indicates very dry environmental conditions with strongly reduced soil humidity. Since such results strongly challenge the interpretation based on *n*-alkane patterns, more future activities are required to derive independent proxy data from the LPSs in order to achieve a valid reconstruction of paleoenvironmental conditions.

3.4.3. Grasses and Herbs as Indicators of Humid Conditions Rather Than of Drier Ones

A closer look to the pedocomlex (P-1) reveals that total *n*-alkane concentrations increased in correlation with a changeover of soil properties. Starting from a coarsely aggregated brown soil, leading to a black-brown soil, and finally to a crumbly pure black soil (steppe soil), an increasing TAC points to higher production and/or better preservation of alkanes under steppic conditions. The fact that appearance and characteristics of the brown paleosoils at the base of P-1 give evidence of intense weathering fits well with the indication of stronger alkane degradation in these paleosoils. However, the ACL did not change noticeably within the pedocomplex. Since the ACL and further alkane ratios indicate grass-dominated vegetation cover across all soils of the pedocomplex, the following conclusions may be drawn. As soon as environmental conditions became slightly wetter, incipient pedogenesis has been accompanied by the establishment of steppe vegetation that is indicated by the increase of grass-derived *n*-alkanes. Probably there was hardly any forest composed of deciduous trees, instead, high grasses dominated. For the last interglacial period, certain indications of tree vegetation were detected such as the filled root channels, but the observed *n*-alkane signal still refers to predominant grass vegetation. A forest steppe environment may explain such findings because the biomass of grasses and herbs might be remarkably higher thanks to a longer growing season and higher growth rates compared with biomass produced by trees [63]. In the same direction, likewise, pollen analyses that were conducted in sediments of the Shamb paleo-lake in southern Armenia [5], demonstrate that steppe elements were always abundant at Shamb, even during interglacial periods and nowadays.

Later, when it became drier during glacial/stadial periods, a transition from humid grass biome to semi-desert shrub communities may have taken place, leading to the production of alkanes with the dominant chain length nC_{29} (probably nC_{27}, too). An ecological state transition from grasslands to dominated shrublands ecosystem are very common in arid regions nowadays (in Armenia too) and are usually attributed to various factors relating to pronounced aridity and limited precipitation [70–72]. With increased aridity there is a competition between grasses and shrubs. Certain shrubs have the ability to perform photosynthesis for a longer period of the growing season thanks to deep and laterally-extensive root systems that access deeper groundwater [73]. This limits the establishment of grass vegetation and promotes the growth of semi-desert shrub species. However, lower temperatures during glacial periods may have exerted considerable stress on shrubs growth, but probably positive temperature feedbacks may have occurred. Some modern research in the Chihuahuan Desert grasslands in the USA focusses on grasses–shrubs transition nowadays and demonstrates an increase of bare soils in shrub biomes. Resulting larger open spaces absorb greater amounts of solar radiation, which is transformed into thermal energy and stored in the ground, and later warms up the near-surface air layer close to the shrublands [74,75]. The authors show that increased nocturnal air temperatures may reduce juvenile mortality and favor continuing shrub growth and survival during cold periods [74,76].

To summarize, patterns of *n*-alkane production in NE-Armenian LPSs might indicate a transition from humid high steppe biome or forest steppe occurring during periods of soil formation (interglacial/interstadial) to semi-desert shrub species more adapted to enhanced aridity during

glacial periods. This also implies that *n*-alkane-based grass signals may be seen as an indication of more humid environmental conditions, rather than of dry conditions as widely supposed.

4. Conclusions

Within this study, *n*-alkane biomarker analyses were applied to modern plants and top soils, as well as two recently discovered LPSs in NE-Armenia for the first time. Investigations on modern samples demonstrate that, despite the large interplant variability within vegetation groups that is mainly attributed to changes in local environmental conditions (e.g., changes in temperature and aridity), a promising discrimination power based on nC_{33} (probably nC_{31} as observed in grassland top soils) for grasses and herbs versus nC_{29} for deciduous trees is detected.

The results from Armenian LPSs suggest three hypotheses:

(1) In the same line with recent observations, stressful environments could globally control the production of *n*-alkane patterns and alter the plant's chemotaxonomic character. On the one hand, pronounced irradiation or very dry warm summers might boost the production of the *n*-alkanes chain length nC_{31} and nC_{33}, even by deciduous trees during interglacial periods. On the other hand, a shortening of the *n*-alkane chains produced by grasses and herbs might occur due to the enhanced aridity and temperature decrease during glacial/stadial periods.

(2) The study area may have been an important glacial refuge for deciduous trees leading to tree survival even during glacial periods thanks to higher ecologically effective moisture (i.e., including effects of reduced evapotranspiration). However, recent pollen analysis from a wider Caucasian region together with certain soil and sediment features in Armenian LPS challenge such an interpretation.

(3) A transition took place from humid-steppe biome or forest-steppe vegetation that was dominant during periods of soil formation (interglacial/interstadial) towards aridity-adapted semi-desert shrub species during glacial periods. In that case, *n*-alkane-derived grass signals would not be an indication of dry environmental conditions as widely supposed, but rather of a more humid situation.

At the moment we do prefer the third hypothesis as it seems to be likewise supported by gastropod analyses on the investigated LPS (Richter et al., in prep). The analysis of *n*-alkane biomarkers is still a promising tool to reconstruct paleoenvironmental changes. However, we think that it is very advisable to combine this analysis with the survey of further proxy information such as pollen compositions, land snail assemblages, or isotope measurements (e.g., 15N), in order to boost interpretation.

Supplementary Materials: The following are available online at http://www.mdpi.com/2076-3263/9/6/263/s1, Table S1: modern plant data; Table S2: modern top soils data; Table S3: AJ profile data; Table S4: BL profile data.

Author Contributions: Conceptualization, Y.T., D.W., M.Z., D.F.; methodology, Y.T. and M.Z.; writing—original draft preparation, Y.T.; writing—review and editing, Y.T., D.W., M.Z., R.Z., D.F. and M.F.; supervision, D.F. and D.W.; project administration, D.W. and L.S.; contribution to fieldwork and sampling, D.W., H.H., K.S. and T.W.

Funding: This research was funded by the German research foundation (DFG), FA 239/21-1.

Acknowledgments: We greatly thank Bruno Glaser for providing us lab facilities, Johannes Hepp for support of the laboratory work, and all members of the Soil Biogeochemistry Group at the Martin Luther University Halle-Wittenberg. Furthermore, we thank Christiane Richter (TU-Dresden), Hans von Suchodoletz (University of Leipzig), and Marcel Bliedtner (Friedrich-Schiller-Univerität Jena) for helpful comments and fruitful discussions.

Conflicts of Interest: The authors declare no conflict of interest. The funders had no role in the design of the study; in the collection, analyses, or interpretation of data; in the writing of the manuscript, or in the decision to publish the results.

References

1. Pasoyan, A.; Harytyunyan, D. *Politics of Climate Change in Armenia: Commitments and the International Climate Negotiations*; Heinrich Böll Stiftung: TBLISI South Caucasus region, Georgia; Yerevan, Armenia, 2015.
2. Vardevanyan, A.; Baloyan, S.; Darbinyan, N. *National Action Program on Struggle Against Desertification in Armenia*; Ministry of Nature Protection: Yerevan, Armenia, 2002; p. 193. ISBN 99930-935-6-4. (In Russian)
3. Sayadian, J.V.; Aleshinskaja, Z.V.; Pirumova, L.G.; Rybakova, N.O. On the Age, Interrelations and Conditions of the Formation of Pliocene continental deposits of the Syunik plateau. *Probl. Geol. Quat. Period Armen.* **1983**, 45–59. (In Russian)
4. Bruch, A.; Gabrielyan, I.G. Quantitative data of the Neogene climatic development in Armenia and Nakhichevan. *Acta Univ. Carol. Geol.* **2002**, *46*, 41–48.
5. Joanin, S.; Cornee, J.; Münch, P.; Fornari, M.; Vasiliev, I.; Krijgsman, W.; Nahapetyan, S.; Gabrielyan, I.; Ollivier, V.; Roiron, P.; et al. Early Pleistocene climate cycles in continental deposits of the Lesser Caucasus of Armenia inferred from palynology, magnetostratigraphy and $^{40}Ar/^{39}Ar$ dating. *Earth Planet Sci. Lett.* **2010**, *291*, 149–158. [CrossRef]
6. Leroyer, C.; Joannin, S.; Aoustin, D.; Ali, A.A.; Peyron, O.; Ollivier, V.; Tozalakyan, A.; Karakhanyan, A.; Jude, F. Mid Holocene vegetation from Vanevan peat (south-eastern shore of Lake Sevan, Armenia). *Quat. Int.* **2016**, *395*, 5–18. [CrossRef]
7. Wolf, D.; Baumgart, P.; Meszner, S.; Fülling, A.; Haubold, F.; Sahakyan, L.; Meliksetian, K.; Faust, D. Loess in Armenia stratigraphic findings and paleoenvironmental indications. *Proc. Geol. Assoc.* **2016**, *127*, 29–39. [CrossRef]
8. Buggle, B.; Wiesenberg, G.L.; Glaser, B. Is there a possibility to correct fossil *n*-alkane data for post-sedimentary alteration effects? *Appl. Geochem.* **2010**, *25*, 947–957. [CrossRef]
9. Frechen, M. Loess in Eurasia (special issue). *Quat. Int.* **2011**, *234*, 1–202. [CrossRef]
10. Frechen, M. Loess in Europe (special issue). *EGQSJ* **2011**, *60*, 3–5.
11. Markovic, S.B.; Hambach, U.; Stevens, T.; Kulka, G.; Heller, F.; McCoy, W.D.; Oches, E.A.; Buggle, B.; Zöller, L. The last million years recorded at the Stari Slankamen (Northern Serbia) loess-paleosol sequence: Revised chronostratigraphy and long-term environmental trends. *Quat. Sci. Rev.* **2011**, *30*, 9–10. [CrossRef]
12. Zech, R.; Zech, M.; Markovic, S.; Hambach, U.; Huang, Y. Humid glacials, arid interglacials? Critical thoughts on pedogenesis and paleoclimate-based on multiproxy analyses of the loess-paleosol sequence Cervenka, Northern Serbia. *Palaeogeogr. Palaeoclimatol. Palaeoecol.* **2013**, *387*, 165–175. [CrossRef]
13. Faust, D.; Yanes, Y.; Willkommen, T.; Roettig, C.; Richter, D.; Richter, D.; Suchodoletz, H.V.; Zöller, L. A contribution to the understanding of late Pleistocene Dune sand-Paleosol-Sequences in Fuerteventura (Canary Islands). *Geomorphology* **2015**, *246*, 290–304. [CrossRef]
14. Zhang, Z.; Zhao, M.; Eglinton, G.; Lu, H.; Huang, C.Y. Leaf wax lipids as paleovegetational and paleoenvironmental proxies for the Chinese Loess Plateau over the last 170 kyr. *Quat. Sci. Rev.* **2006**, *25*, 575–594. [CrossRef]
15. Bai, Y.; Fang, X.; Nie, J.; Wang, Y.; Wu, F. A preliminary reconstruction of the paleoecological and paleoclimatic history of the Chinese Loess Plateau from the application of biomarkers. *Palaeogeogr. Palaeoclimatol. Palaeoecol.* **2009**, *271*, 161–169. [CrossRef]
16. Zech, M.; Buggle, B.; Leiber, K.; Markovic, S.; Glaser, B.; Hambach, U.; Huwe, B.; Stevens, T.; Sümegi, P.; Wiesenberg, G.; et al. Reconstructing Quaternary vegetation history in the Carpathian Basin, SE-Europe, using n-alkane biomarkers as molecular fossils: Problems and possible solutions, potential and limitations. *Quat. Sci. J.* **2009**, *2*, 150–157.
17. Zech, M.; Pedentchouk, N.; Buggle, B.; Leiber, K.; Kalbitz, K.; Markovic, S.B.; Glaser, B. Effects of leaf litter degradation and seasonality on D/H isotope ratios of *n*-alkane biomarkers. *Geochim. Cosmochim. Acta* **2011**, *75*, 4917–4928. [CrossRef]
18. Riederer, M.; Schreiber, L. Protecting against water loss analysis of the barrier properties of plant cuticles. *J. Exp. Bot.* **2001**, *52*, 2023–2032. [CrossRef] [PubMed]
19. Post-Beittenmiller, D. Biochemistry and molecular biology of wax production in plants. *Annu. Rev. Plant Biol.* **1996**, *47*, 405–430. [CrossRef]
20. Jetter, R.; Kunst, L.; Samuels, A.L. The composition of plant cuticular waxes. In *Annual Plant Reviews, Biology of the Plant Cuticle*; Blackwell Publishing Ltd.: Hoboken, NJ, USA, 2006.

21. Bargel, H.; Koch, K.; German, Z.; Neinhuis, C. Structure-function relationships of the plant cuticle and cuticular waxes–a smart material. *Funct. Plant Biol.* **2006**, *33*, 893–910. [CrossRef]
22. Eglinton, G.; Hamilton, R.J. Leaf Epicuticular Waxes. *Science* **1967**, *156*, 1322–1335. [CrossRef]
23. Eglinton, T.I.; Eglinton, G. Molecular proxies for paleoclimatology. *EPSL* **2008**, *275*, 1–16. [CrossRef]
24. Cranwell, P.A. Chain-length distribution of *n*-alkanes from lake sediments in relation to post-glacial environmental change. *Freshwater Biol.* **1973**, *3*, 259–265. [CrossRef]
25. Schwark, L.; Zink, K.; Lechterbeck, J. Reconstruction of postglacial to early Holocene vegetation history in terrestrial Central Europe via cuticular lipid biomarkers and pollen records from lake sediments. *Geology* **2002**, *30*, 463–466. [CrossRef]
26. Zech, M. Evidence for Late Pleistocene climate changes from buried soils on the southern slopes of Mt. Kilimanjaro, Tanzania. *Palaeogeogr. Palaeoclimatol. Palaeoecol.* **2006**, *242*, 303–312. [CrossRef]
27. Schäfer, I.K.; Lanny, V.; Franke, J.; Eglinton, T.I.; Zech, M.; Vysloužilová, B.; Zech, R. Leaf waxes in litter and topsoils along a European transect. *SOIL* **2016**, *2*, 551–564. [CrossRef]
28. Bush, R.T.; Mc Inerney, F.A. Leaf wax n-alkane distributions in and across modern plants: Implications for paleoecology and chemotaxonomy. *Geochim. Cosmochim. Acta* **2013**, *117*, 161–179. [CrossRef]
29. Encyclopaedia Britannica. Available online: https://www.britannica.com/place/Armenia (accessed on 23 April 2019).
30. Chorbajian, S.A. *Deforestration in the Republic of Armenia: A Human and Environmental Crisis*; Bard College: New York, NY, USA, 2006.
31. Hergnyan, Y.; Hovhannisyan, S.; Grigaryan, S.; Sayadyan, H. *The Economics of Armenia Forest Industry*; Economy and values research center: Yerevan, Armenia, 2007.
32. Ziroyan, R. Conversation and sustainable use of forest in Armenia. In Proceedings of the XII Word Forestry Congress, Quebec City, QC, Canada, 21–28 September 2003.
33. Bohn, U.; Zazanashvili, N.; Nakhutsrishvili, G. The Map of the Natural Vegetation of Europe and its application in the Caucasus Ecoregion. *Bull. Georgian Natl. Acad. Sci.* **2007**, *175*, 112–121.
34. Diefendorf, A.F.; Freeman, K.H.; Wing, S.L.; Graham, H.V. Production of n-alkyl lipids in living plants and implications for the geologic past. *Geochim. Cosmochim. Acta* **2011**, *75*, 7472–7485. [CrossRef]
35. Zech, R.; Gao, L.; Tarozo, R.; Huang, Y. Branched glycerol dialkyl glycerol tetraethers in Pleistocene loess-paleosol sequences: Three case studies. *Org. Geochem.* **2012**, *53*, 38–44. [CrossRef]
36. Hoefs, M.J.; Rijpstra, W.C.; Sinninghe Damsté, J.S. The influence of degradation on the sedimentary biomarker record: Evidence from Madeira Abyssal Plain turbidites. *Geochim. Cosmochim. Acta* **2002**, *66*, 2719–2735. [CrossRef]
37. Poynter, J.G.; Farrimond, P.; Robinson, N.; Eglinton, G. Aeolian Derived Higher Plant Lipids in the Marine Sedimentary Record: Links with Palaeoclimate. In *Paleoclimatology and Paleometeorology: Modern and Past Patterns of Global Atmospheric Transport*; Leinen, M., Sarnthein, M., Eds.; Springer: Dordrecht, The Netherlands, 1989; pp. 435–462.
38. Bush, R.T.; McInerney, F.A. Influence of temperature and C4 abundance on *n*-alkane chain length distributions across the central USA. *Org. Geochem.* **2015**, *79*, 65–73. [CrossRef]
39. Feakins, S.J.; Peters, T.; Wu, M.S.; Shenkin, A.; Salinas, N.; Girardin, C.A.; Bentley, L.P.; Blonder, B.; Enquist, B.J.; Martin, R.E.; et al. Production of leaf wax n-alkanes across a tropical forest elevation transect. *Org. Geochem.* **2016**, *100*, 89–100. [CrossRef]
40. Rao, Z.; Wu, Y.; Zhu, Z.; Jia, G.; Henderson, A. Is the maximum carbon number of long-chain n-alkanes an indicator of grassland or forest? Evidence from surface soils and modern plants. *Chin. Sci. Bull.* **2011**, *56*, 1714–1720. [CrossRef]
41. Huang, Y.; Lockheart, M.J.; Collister, J.W.; Eglinton, G. Molecular and isotopic biogeochemistry of the Miocene Clarkia formation: Hydrocarbons and alcohols. *Org. Geochem.* **1995**, *23*, 785–801. [CrossRef]
42. Tipple, B.J.; Pagani, M. Environmental control on eastern broadleaf forest species' leaf wax distributions and D/H ratios. *Geochim. Cosmochim. Acta* **2013**, *111*, 64–77. [CrossRef]
43. Vogts, A.; Schefuß, E.; Badewein, T.; Rullkötter, J. N-Alkane parameters from a deep-sea sediment transect off southwest Africa reflect continental vegetation and climate conditions. *Org. Geochem.* **2012**, *47*, 109–119. [CrossRef]
44. Wang, N.; Zong, Y.; Brodie, C.; Zheng, Z. An examination of the fidelity of n-alkanes as a palaeoclimate proxy from sediments of Palaeolake Tianyang, South China. *Quat. Int.* **2014**, *333*, 100–109. [CrossRef]

45. Kirkels, F.; Jansen, B.; Kalbitz, K. Consistency of plant-specific *n*-alkane patterns in plaggen ecosystems. *Holocene* **2013**, *23*, 1355–1368. [CrossRef]
46. Janson, B.; Nierop, K.G.J.; Hageman, J.A.; Cleef, A.M.; Verstraten, J.M. The straight lipid biomarker composition of plant species responsible for the dominant biomass production along two altitudinal transects in the Ecuadorian Andes. *Org. Geochem.* **2006**, *37*, 1514–1536. [CrossRef]
47. Naafs, D.F.; Van Bergen, P.F.; Boogert, S.J.; De Leeuw, J.W. Solvent extractable lipids in an acid andic forest soil; variation with depth and season. *Soil Biol. Biochem.* **2004**, *36*, 297–308. [CrossRef]
48. Meyers, P.A.; Ishiwatari, R. Lacustrine organic geochemistry an overview of indicators of organic matter sources and diagenesis in lake sediments. *Org. Geochem.* **1993**, *20*, 867–900. [CrossRef]
49. Bliedtner, M.; Schäfer, I.; Zech, R.; Von Suchodoletz, H. Leaf wax n-alkanes in modern plants and topsoils from eastern Georgia (Caucasus) implications for reconstructing regional paleo-vegetation. *Biogeosciences* **2017**, *15*, 3927–3936. [CrossRef]
50. Dodd, R.S.; Poveda, M.M. Environmental gradients and population divergence contribute to variation in cuticular wax composition in *Juniperus communis*. *Biochem. Syst. Ecol.* **2003**, *31*, 1257–1270. [CrossRef]
51. Vogts, A.; Moossen, H.; Rommerskirchen, F.; Rullkötter, J. Distribution patterns and stable carbon isotopic composition of alkanes and alkaloids from plant waxes of the African rain forest and savanna C3 species. *Org. Geochem.* **2009**, *40*, 1037–1054. [CrossRef]
52. Shepherd, T.; Wynne Griffiths, D. The effects of stress on plant cuticular waxes. *New Phytol.* **2006**, *171*, 469–499. [CrossRef] [PubMed]
53. Gülz, P.G. Epicuticular leaf waxes in the evolution of the plant. Kingdom. *Plant Physiol.* **1994**, *143*, 453–464. [CrossRef]
54. Lockheart, M.J.; Van Bergen, P.F.; Everhard, R.P. Variations in the stable carbon isotope compositions of individual lipids from the leaves of modern angiosperms: Implications for the study of higher land-plant derived sedimentary organic matter. *Org. Geochem.* **1997**, *26*, 137–153. [CrossRef]
55. Tu, T.T.N.; Egasse, C.; Zeller, B.; Bardoux, G.; Biron, P.; Ponge, J.F.; David, B.; Derenne, S. Early degradation of plant alkanes in soils: A little bag experience using ^{13}C-labelled leaves. *Soil Biol. Biochem.* **2011**, *43*, 2222–2228.
56. Sachse, D.; Radke, J.; Gleixner, G. δD values of individual *n*-alkanes from terrestrial plants along a climatic gradient. Implications for the sedimentary biomarker record. *Org. Geochem.* **2006**, *37*, 469–483. [CrossRef]
57. Guo, N.; Gao, J.; He, Y.; Zhang, Z.; Guo, Y. Variations in leaf epicuticular n-alkanes in some Broussonetia, Ficus and Humulus species. *Biochem. Syst. Ecol.* **2014**, *54*, 150–156. [CrossRef]
58. Schulz, S.; Giebler, J.; Chatzinotas, A.; Wick, L.Y.; Fetzer, I.; Welzl, G.; Harms, H.; Schloter, M. Plant litter and soil type drive abundance, activity and community structure of alkB harbouring microbes in different soil compartments. *ISME J.* **2012**, *6*, 1763–1774. [CrossRef] [PubMed]
59. Zech, M.; Krause, T.; Meszner, S.; Faust, D. Incorrect when incorrect: Reconstructing vegetation history using *n*-alkane biomarkers in loess-paleosol sequences- A case study from the Saxonian loess region, German. *Quat. Int.* **2013**, *296*, 108–116. [CrossRef]
60. Schatz, A.K.; Zech, M.; Buggle, B.; Gulyás, S.; Hambach, U.; Markovic, S.B.; Sümegi, P.; Scholten, T. The late Quaternary loess record of Tokaj, Hungary: Reconstructing palaeoenvironment, vegetation and climate using stable C and N isotopes and biomarkers. *Quat. Int.* **2011**, *240*, 52–61. [CrossRef]
61. Rinna, J.; Gunter, U.; Hinrichs, K.U.; Mangelsdorf, K.; Van der Smissen, J.H.; Rullkotter, J. Temperature related molecular proxies: Degree of alkenone unsaturation and average chain length of n-alkanes. In *Proceedings of the Sixteenth Annual Pacific Climate Workshop*; The Wrigley Institute for Environmental Studies: Two Harbors, Santa Catalina Island, CA, USA, 1999.
62. Obreht, I.; Zeeden, C.; Hambach, U.F.; Markovic, S. A critical reevaluation of Paleoclimate proxy records from Loess in the Carpathian basin. *Earth Sci. Rev.* **2019**, *190*, 498–520. [CrossRef]
63. Panagiotopoulos, K.; Aufgebauer, A.; Schäbitz, F.; Wagner, B. Vegetation and climate history of the Lake Prespa region since the Late glacial. *Quat. Int.* **2013**, *293*, 157–169. [CrossRef]
64. Tzedakis, P.C.; Hooghiemstra, H.; Pälike, H. The last 1.35 million years at Tenaghi Philippon: Revised chronostratigraphy and long-term vegetation trends. *Quat. Sci. Rev.* **2006**, *25*, 3416–3430. [CrossRef]
65. Pakhomov, M.M. Glacial-Interglacial cycles in arid regions of northern Eurasia. *Quat. Int.* **2006**, *152*, 70–77. [CrossRef]

66. Messager, E.; Lordkipanidze, D.; Ferring, C.R.; Deniaux, B. Fossil fruit identification by SEM investigations, a tool for palaeoenvironmental reconstruction of Dmanisi site, Georgia. *J. Archaeol. Sci.* **2008**, *35*, 2715–2725. [CrossRef]
67. Djamali, M.; De Beaulieu, J.-L.; Shah-hosseini, M.; Andrieu-Ponel, V.; Ponel, P.; Amini, A.; Akhani, H.; Leroy, S.A.G.; Stevens, L.; Lahijani, H.; et al. A Late Pleistocene long pollen record from Lake Urmia, NW Iran. *Quat. Res.* **2008**, *69*, 413–420. [CrossRef]
68. Pickarski, N.; Kwiecien, O.; Djamali, M.; Litt, T. Vegetation and environmental changes during the last interglacial in eastern Anatolia (Turkey): A new high-resolution pollen record from Lake Van. *Palaeogeogr. Palaeoclimatol. Palaeoecol.* **2015**, *435*, 145–158. [CrossRef]
69. Pickarski, N.; Litt, T. A new high resolution pollen sequence at Lake Van, Turkey: Insight into penultimate interglacial- glacial climate change on vegetation history. *Clim. Past* **2017**, *13*, 689–710. [CrossRef]
70. Archer, S.; Schimel, D.S.; Holland, E.A. Mechanisms of shrubland expansion: Land use, climate or CO_2. *Clim. Chang.* **1995**, *29*, 91–99. [CrossRef]
71. Van Auken, O.W. Shrub invasions of North American semiarid grasslands. *Annu. Rev. Ecol. Evol. Syst.* **2000**, *31*, 197–215. [CrossRef]
72. Ravi, S.; D'Odorico, P.; Collins, S.L.; Huxman, T.E. Can biological invasions induce desertification? *New Phytol.* **2009**, *181*, 512–515. [CrossRef] [PubMed]
73. Gile, L.H.; Gibbens, R.P.; Lenz, J.M. The near-ubiquitous pedogenic world of mesquite roots in an arid basin floor. *J. Arid Environ.* **1997**, *35*, 39–58. [CrossRef]
74. He, Y.F.; D'Odorico, P.; De Wekker, S.F.J.; Fuentes, J.D.; Litvak, M. On the impact of shrub encroachment on microclimate conditions in the northern Chihuahuan desert. *J. Geophys. Res. Atmos.* **2010**, *115*, D21120. [CrossRef]
75. Huenneke, L.F.; Anderson, J.P.; Remmenga, M.; Schlesinger, W.H. Desertification alters patterns of aboveground net primary production in Chihuahuan ecosystems. *Global Chang. Biol.* **2002**, *8*, 247–264. [CrossRef]
76. D'odorico, P.; Okin, G.S.; Bestelmeyer, B.T. A synthetic review of feedbacks and drivers of shrub encroachment in arid grassland. *Ecohydrology* **2012**, *5*, 520–530. [CrossRef]



© 2019 by the authors. Licensee MDPI, Basel, Switzerland. This article is an open access article distributed under the terms and conditions of the Creative Commons Attribution (CC BY) license (http://creativecommons.org/licenses/by/4.0/).